NLRP2 controls age-associated maternal fertility

Anna A. Kuchmiy,[1,2] Jinke D'Hont,[1,3] Tino Hochepied,[1,3] and Mohamed Lamkanfi[1,2]

[1]Inflammation Research Center, VIB, B-9052 Zwijnaarde, Belgium
[2]Department of Internal Medicine and [3]Department of Biomedical Molecular Biology, Ghent University, B-9000 Ghent, Belgium

Nucleotide-binding domain and leucine-rich repeat (NLR) proteins are well-known for their key roles in the immune system. Ectopically expressed NLRP2 in immortalized cell lines assembles an inflammasome and inhibits activation of the proinflammatory transcription factor NF-κB, but the physiological roles of NLRP2 are unknown. Here, we show that Nlrp2-deficient mice were born with expected Mendelian ratios and that Nlrp2 was dispensable for innate and adaptive immunity. The observation that Nlrp2 was exclusively expressed in oocytes led us to explore the role of Nlrp2 in parthenogenetic activation of oocytes. Remarkably, unlike oocytes of young adult Nlrp2-deficient mice, activated oocytes of mature adult mice developed slower and largely failed to reach the blastocyst stage. In agreement, we noted strikingly declining reproductive rates in vivo with progressing age of female Nlrp2-deficient mice. This work identifies Nlrp2 as a critical regulator of oocyte quality and suggests that *NLRP2* variants with reduced activity may contribute to maternal age-associated fertility loss in humans.

INTRODUCTION

Nucleotide-binding domain and leucine-rich repeat (NLR) proteins are well-established hub proteins regulating a diversity of inflammatory and host defense responses in the immune system. Class II major histocompatibility complex transactivator (CIITA), nucleotide-binding oligomerization domain receptor 1 (NOD1), and NOD2 are founding family members that, respectively, control MHC-II transcription and peptidoglycan-induced NF-κB and MAP kinase activation, whereas NLRC5 regulates MHC-I gene expression (Kanneganti et al., 2007; Ting et al., 2008; Geddes et al., 2009; Lupfer and Kanneganti, 2013). Another subset of NLRs plays central roles in the assembly of inflammasomes, multiprotein scaffolds that couple direct and indirect detection of pathogen- and danger-associated molecular patterns to recruitment and activation of the prototype inflammatory caspase-1 for production of bioactive IL-1β and IL-18. We distinguish the Nlrp1a and Nlrp1b, Nlrp3, and Nlrc4 inflammasomes, among several other emerging inflammasomes (Lamkanfi and Dixit, 2014). The NLRP1a inflammasome currently lacks a defined activating agent, but bacterial pathogens such as *Salmonella enterica* serovar Typhimurium, *Pseudomonas aeruginosa*, *Legionella pneumophila*, and *Shigella flexneri* all engage the NAIP/Nlrc4 inflammasome. The Nlrp1b inflammasome is triggered by anthrax lethal toxin (LeTx). Finally, the Nlrp3 inflammasome reacts to a broad range of bacterial, viral, and fungal pathogens, as well as danger-associated molecular patterns linked to autoimmune diseases (Lamkanfi and Dixit, 2012).

Unlike the aforementioned NLRs, the roles of NLRP2 are ill-defined. Ectopically expressed NLRP2 was shown to regulate inflammasome signaling and to inhibit NF-κB activation (Agostini et al., 2004; Bruey et al., 2004; Kinoshita et al., 2005; Fontalba et al., 2007). Knockdown studies have also suggested Nlrp2 to be essential for early mouse embryogenesis (Peng et al., 2012). Despite these advances, the physiological roles of Nlrp2 are unknown. Here, we describe Nlrp2-deficient mice and report that Nlrp2 deletion altered neither innate nor adaptive immune responses in ex vivo–stimulated leukocytes and in in vivo–challenged mice. However, we identified a role for oocyte-expressed Nlrp2 in early embryogenesis and show that Nlrp2 contributed importantly to in vivo fertility with progressing maternal age. Thus, this work highlights Nlrp2 as a critical and selective regulator of oocyte quality, suggesting that *NLRP2* variants with reduced activity may contribute to maternal age-associated fertility loss in humans.

RESULTS AND DISCUSSION

Nlrp2 is dispensable for innate and adaptive immunity

To study the in vivo roles of Nlrp2, we generated Nlrp2-deficient mice by flanking exon 5—which encodes most of the central NACHT ATPase domain—with LoxP sites to allow Cre recombinase-assisted conditional deletion of the targeted exon (Fig. S1). Surprisingly, full-body $Nlrp2^{-/-}$ mice were born from heterozygous parents with expected Mendelian ratios, and no phenotypic abnormalities were noted (Table S1). To probe for putative roles of Nlrp2 in inflammasome regulation, we assessed IL-1β secretion from LPS-primed $Nlrp2^{-/-}$ and WT BM-derived macrophages

Correspondence to Mohamed Lamkanfi: mohamed.lamkanfi@irc.vib-ugent.be

Abbreviations used: BMDM, BM-derived macrophage; CIITA, class II major histocompatibility complex transactivator; ES, embryonic stem; FRT, FLP recombinase target; LDH, lactate dehydrogenase; LeTx, lethal toxin; NLR, nucleotide-binding domain and leucine-rich repeat containing protein family; NOD, nucleotide-binding oligomerization domain receptor.

The Rockefeller University Press $30.00
J. Exp. Med. 2016 Vol. 213 No. 13 2851–2860
https://doi.org/10.1084/jem.20160900

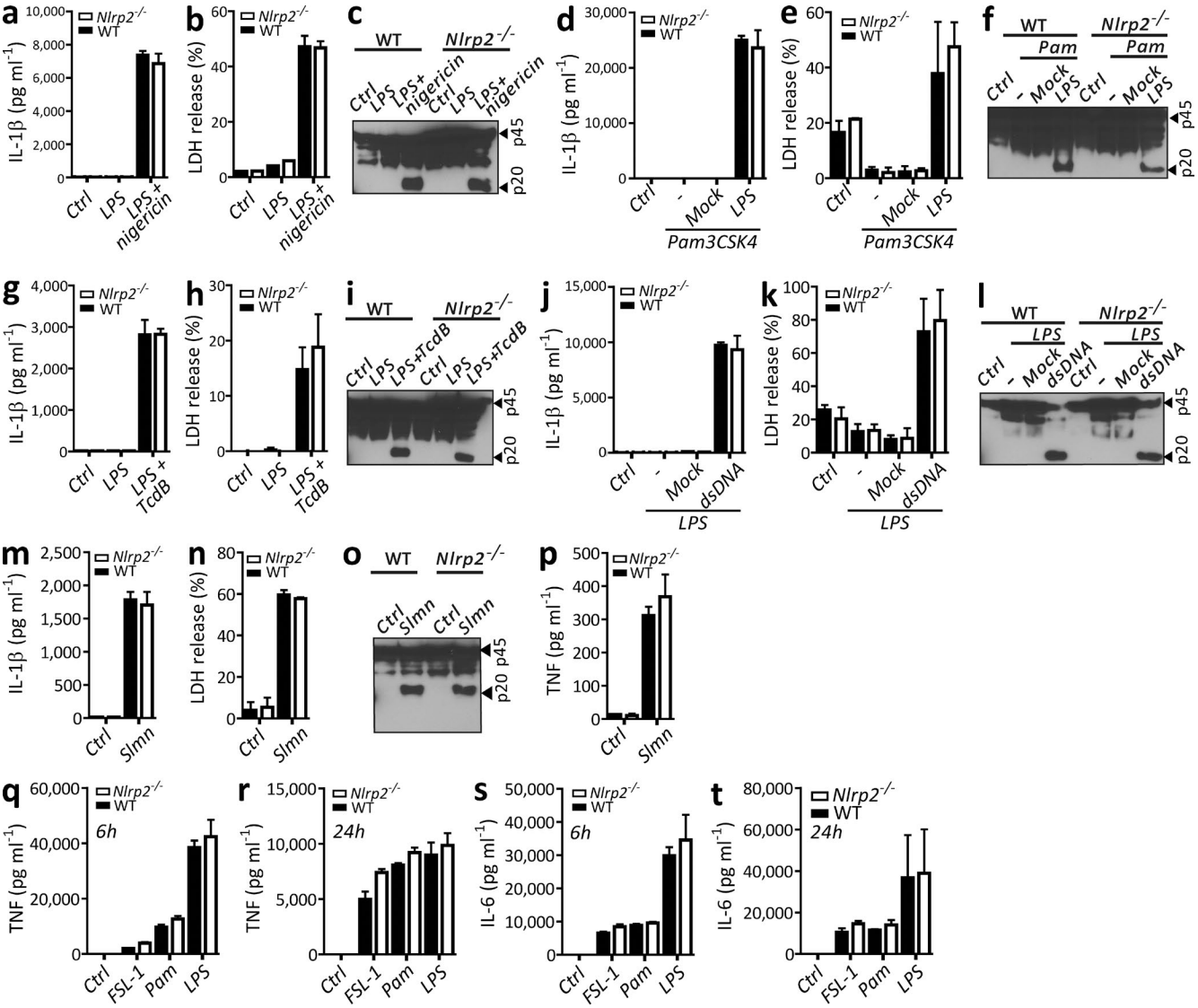

Figure 1. **Nlrp2 deficiency alters neither inflammasome activation nor TLR-dependent cytokine production.** (a–c) WT and *Nlrp2*$^{-/-}$ BMDMs were left untreated (ctrl) or primed with 0.5 µg ml^{-1} LPS for 2 h. In some setups, cells were then stimulated with 20 µM nigericin for 45 min. (d–f) WT and *Nlrp2*$^{-/-}$ BMDMs were left untreated or primed with the TLR2 ligand Pam3CSK4, and subsequently transfected with vehicle control or ultrapure LPS for 18 h. (g–i) WT and *Nlrp2*$^{-/-}$ BMDMs were left untreated or primed with 0.5 µg ml^{-1} LPS for 2 h. In some setups, cells were subsequently treated with *Clostridium difficile* toxin B (TcdB; 1 µg ml^{-1}) for 5 h. (j–l) WT and *Nlrp2*$^{-/-}$ BMDMs were left untreated or primed with 0.5 µg ml^{-1} LPS for 2 h. Cells were subsequently left untreated or transfected with either vehicle control (mock) or dsDNA for 19 h. (m–o) WT and *Nlrp2*$^{-/-}$ BMDMs were left untreated or infected with *Salmonella* Typhimurium (MOI 5) for 3 h. Supernatants were analyzed for IL-1β (a, d, g, j, and m) and LDH (b, e, h, k, and n), and lysates were immunoblotted for caspase-1 (c, f, i, l, and o). (p) WT and *Nlrp2*$^{-/-}$ BMDMs were left untreated or infected with *Salmonella* Typhimurium (MOI 5) for 3 h before supernatants were collected and analyzed for secreted TNF. (q–t) WT and *Nlrp2*$^{-/-}$ BM-derived DCs were left untreated or stimulated with FSL-1, Pam3CSK4, or LPS (0.1 µg ml^{-1}) for 6 or 24 h. Supernatants were analyzed for TNF (q and r) and IL-6 (s and t). Black arrows on Western blots denote procaspase-1 and the p20 subunit. Data are representative of results from three independent experiments, and cytokine and LDH data are presented as mean ± SD from a single representative experiment, with each condition performed in triplicate. Statistical significance was determined by Student's *t* test; $P < 0.05$ was considered statistically significant.

(BMDMs) after exposure to the canonical Nlrp3 inflammasome stimulus nigericin. The levels of IL-1β detected in culture supernatants of *Nlrp2*$^{-/-}$ macrophages were indistinguishable from those of WT BMDMs (Fig. 1 a). In agreement, pyroptosis (Fig. 1 b) and nigericin-induced caspase-1 maturation (Fig. 1 c) were unaffected. Moreover, activation of neither the noncanonical Nlrp3 inflammasome (Fig. 1, d–f) nor that of other canonical inflammasomes was altered in *Nlrp2*$^{-/-}$ macrophages in terms of IL-1β secretion, caspase-1 maturation, and pyroptosis induction (Fig. 1, g–o).

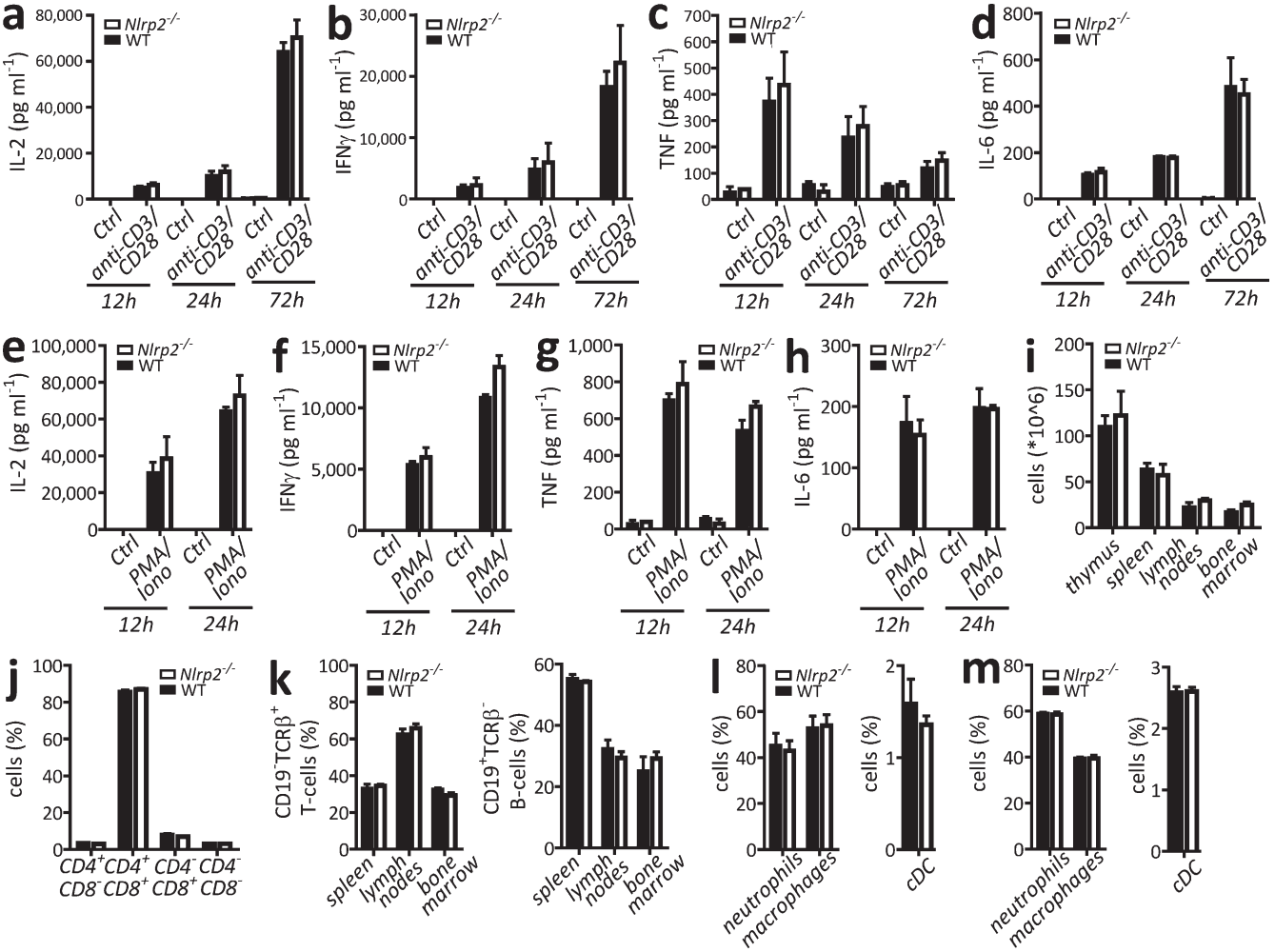

Figure 2. **CD4⁺ T cell responses are not modulated by Nlrp2 deficiency.** (a–h) WT and *Nlrp2*$^{-/-}$ CD4⁺ T cells were left untreated or treated with anti-CD3 (4 µg ml^{-1}; plate-bound) and anti-CD28 (1 µg ml^{-1}) monoclonal antibodies (a–d), or treated with phorbol 12-myristate 13-acetate (PMA; 100 ng ml^{-1}) and ionomycin (1 µg ml^{-1}) for the indicated durations (e–h). Supernatants were analyzed for secretion of IL-2 (a and e), IFN-γ (b and f), TNF (c and g), and IL-6 (d and h). (i) Cellularity of primary and secondary immune organs of naive WT and *Nlrp2*$^{-/-}$ mice. (j) The fraction of immune cell subsets in thymus of naive WT and *Nlrp2*$^{-/-}$ mice was determined. Cells were defined as CD4⁺CD8⁻, CD4⁺CD8⁺, CD4⁻CD8⁺, or CD4⁻CD8⁻. (k) The fraction of CD19⁻TCRβ⁺ T (right) cells and CD19⁺TCRβ⁻ B cells (left) in spleen, lymph nodes, and BM of naive WT and *Nlrp2*$^{-/-}$ mice was determined. (l) Myeloid cell subsets in spleen of naive WT and *Nlrp2*$^{-/-}$ mice were determined. Cells were gated as CD11b⁺CD11c⁻Gr1^{high} neutrophils and CD11b⁺CD11c⁻Gr1$^{low/neg}$ macrophages (left), or as CD11b⁺CD11c⁺ conventional DCs (right). (m) Myeloid cell subsets in BM of naive WT and *Nlrp2*$^{-/-}$ mice were determined. Cells were gated as CD11b⁺CD11c⁻Gr1^{high} neutrophils and CD11b⁺CD11c⁻Gr1$^{low/neg}$ macrophages (left), or as CD11b⁺CD11c⁺ conventional DCs (right). Analyses were performed on at least three mice/genotype. Data are representative of results from at least two independent experiments, and cytokine data are presented as mean ± SD from a single representative experiment, with each condition performed in triplicate. Statistical significance was determined by Student's *t* test; $P < 0.05$ was considered statistically significant.

Together, these results indicate that Nlrp2 is dispensable for known inflammasome pathways.

Although ectopically expressed Nlrp2 inhibited activation of the proinflammatory transcription factor NF-κB (Bruey et al., 2004; Kinoshita et al., 2005; Fontalba et al., 2007), we found that production levels of the NF-κB–dependent cytokine TNF in *Salmonella* Typhimurium–infected macrophages were not modulated by Nlrp2-deficiency (Fig. 1 p). Nor did we detect differential levels of TNF and IL-6 in Nlrp2-sufficient and -deficient DCs that have been stimulated for 6 or 24 h with the TLR2 ligands FSL-1 and Pam3CSK4 or the TLR4 ligand LPS, respectively (Fig. 1, q–t).

Given that Nlrp2 appeared to be negligible for regulation of the examined inflammasome and TLR-induced NF-κB signaling pathways, we sought to more broadly address the role of Nlrp2 in the immune system. To this end, we selectively ablated Nlrp2 expression in the hematopoietic compartment by breeding *Nlrp2*$^{flox/flox}$ mice to mice expressing the Cre recombinase under control of the mouse HS21/45-vav control regions. CD4⁺ T lymphocytes were collected and stimulated

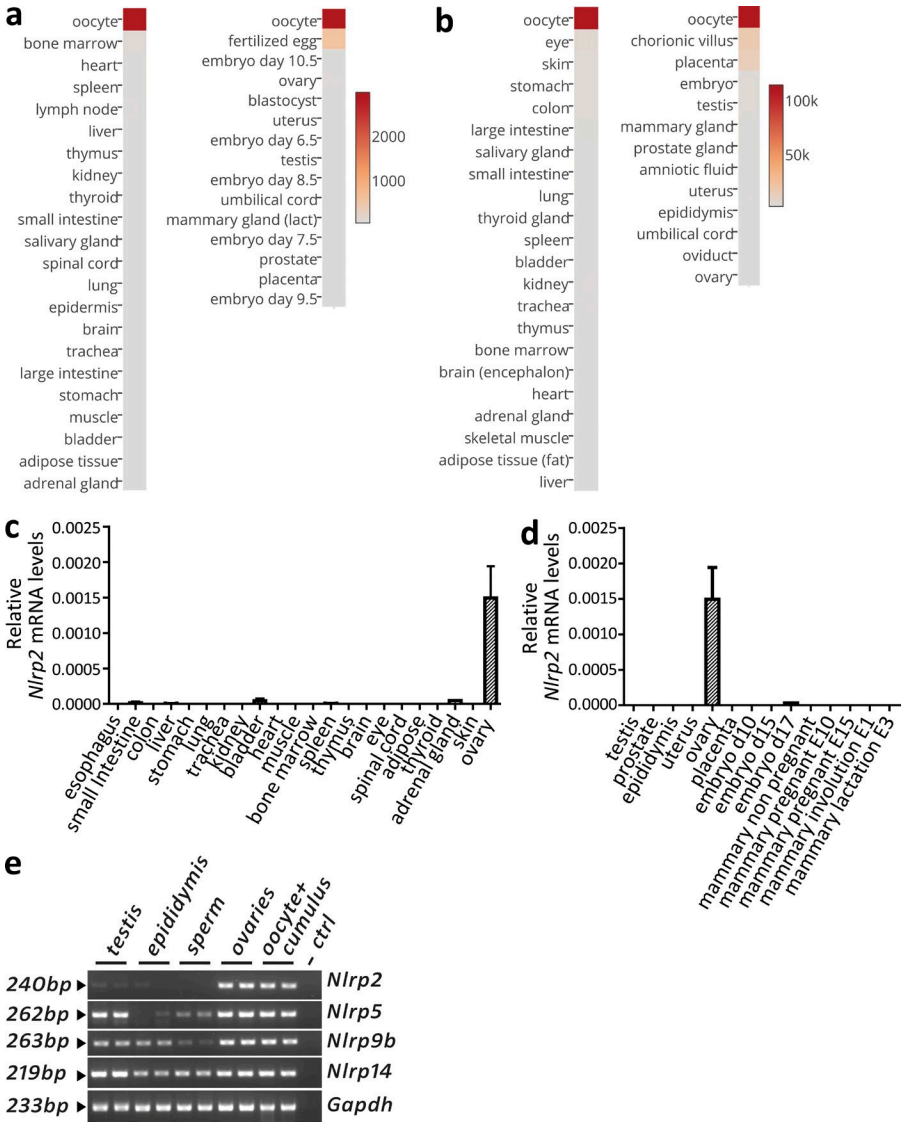

Figure 3. **Murine Nlrp2 is selectively expressed in oocytes.** (a and b) Heat maps depicting expression levels of Nlrp2 mRNA across somatic (left) and reproductive (right) tissues and cell types in mice (a) and humans (b). Mouse Nlrp2 expression levels were retrieved from the Gene Expression Omnibus repository (accession code: GDS592); human data were obtained from Genevestigator; heat maps were built in Plotly software. Red indicates maximal, and gray minimal expression. Red indicates maximal, and gray minimal expression. (c and d) qRT-PCR analysis of Nlrp2 expression levels normalized to Gapdh across murine somatic (c) and reproductive (d) organs and tissues. (e) RT-PCR analysis of murine *Nlrp2*, *Nlrp5*, *Nlrp9b*, and *Nlrp14* expression in male and female reproductive cells and tissues. Gapdh was included for normalization. Data are representative of at least three independent repeats.

ex vivo with anti-CD3 and anti-CD28 monoclonal antibodies to mimic stimulation by antigen-presenting cells. This treatment regimen triggered *Nlrp2*$^{-/-}$ CD4^{+} T cells to produce the hallmark cytokines IL-2 and IFN-γ, as well as TNF and IL-6, with similar potency to WT CD4^{+} T cells (Fig. 2, a–d). Nlrp2 deficiency also failed to modulate T cell receptor–independent cytokine production and lymphocyte proliferation in CD4^{+} T lymphocytes that have been treated with PMA and ionomycin (Fig. 2, e–h). In vivo immunophenotyping further revealed normal distribution profiles of lymphocyte and myeloid cell fractions in thymus, spleen, lymph nodes, and BM of unchallenged full-body *Nlrp2*$^{-/-}$ mice (Fig. 2, i–m). Moreover, *Nlrp2*$^{-/-}$ mice had normal in vivo T cell responses in the NP-KLH in alum immunization model, and expected lethality rates in the LPS-endotoxemia model (unpublished data). Together, these findings suggest that unlike many other NLR family members, Nlrp2 is dispensable for innate and adaptive immunity.

Nlrp2 is uniquely expressed in oocytes

In seeking to define the physiological role of Nlrp2, we characterized its mRNA expression profile in different organs. In agreement with reported findings (Peng et al., 2012), a query of public microarray data revealed abundant expression of Nlrp2 mRNA in oocytes, whereas a variety of other murine tissues and cell types returned negative for Nlrp2 expression (Fig. 3 a). A similar oocyte-restricted expression profile emerged from probing human expression data (Fig. 3 b). Quantitative RT–PCR analysis confirmed the selective expression of Nlrp2 in ovaries (containing oocytes), and its absence in the male reproductive system and somatic tissues of the mouse (Fig. 3, c and d). Several other NLR family members with oocyte expression have been reported (Tong et al., 2000; Peng et al., 2012, 2015), but unlike *Nlrp2*, transcripts of *Nlrp5*, *Nlrp9b*, and *Nlrp14* were also abundantly expressed in the male reproductive system (testis, epididymis, and sperm;

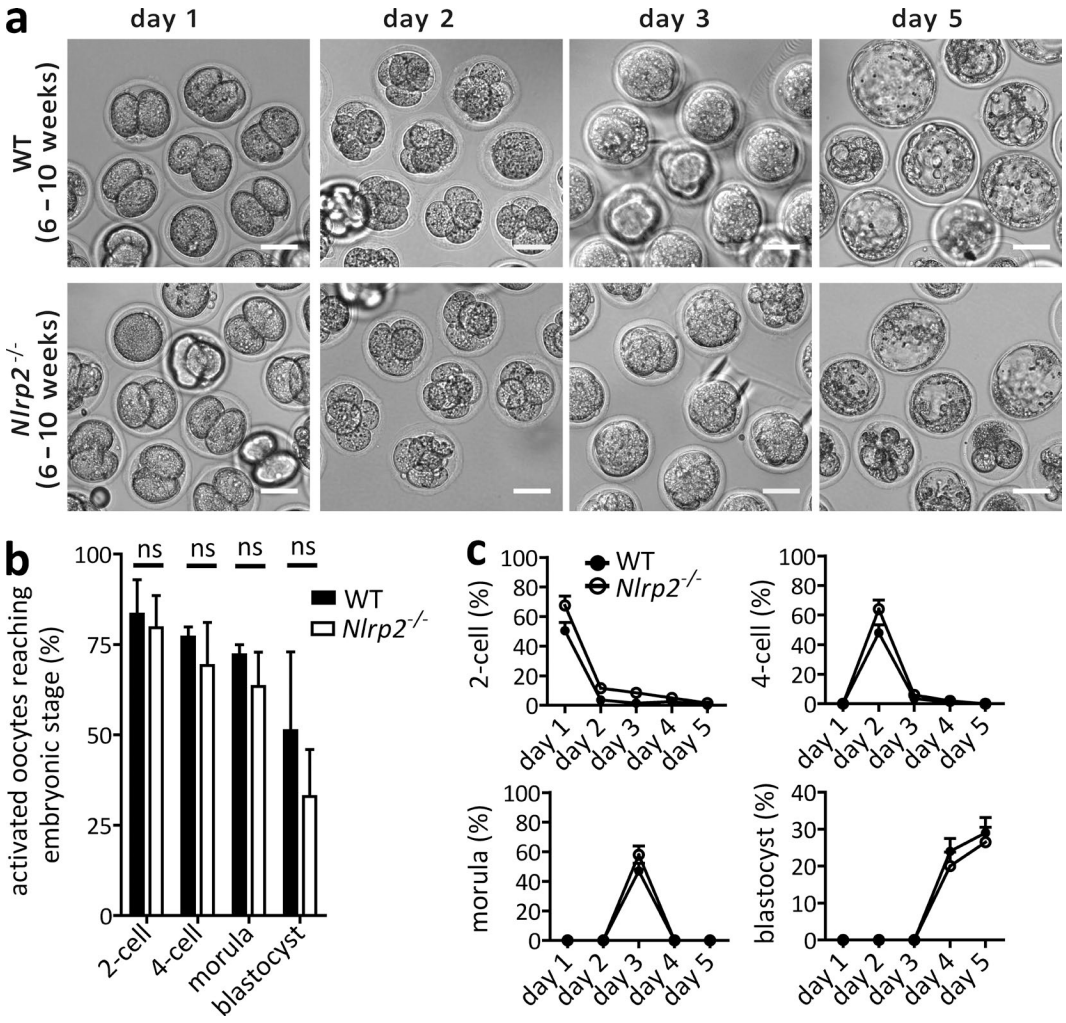

Figure 4. **Nlrp2 is dispensable for parthenogenetic development of oocytes from young adult mice.** (a) Representative bright field micrographs of developing embryos at days 1, 2, 3, and 5 after parthenogenetic activation of oocytes obtained from 6–10-wk-old WT and *Nlrp2*$^{-/-}$ mice. (b) Fraction of activated oocytes from 6–10 wk old WT and *Nlrp2*$^{-/-}$ mice that reached the indicated embryonic cleavage stages. (c) Kinetic analysis of the progression of activated oocytes from 6–10-wk-old WT and *Nlrp2*$^{-/-}$ mice through the indicated embryonic cleavage stages. Data represent mean ± SD of 201 oocytes from 16 WT mice, and 297 oocytes from 16 *Nlrp2*$^{-/-}$ mice. (ns, nonsignificant; Student's *t* test). Bars, 50 µm.

Fig. 3 e). Together, these results suggest that Nlrp2 expression largely is confined to oocytes.

Defective parthenogenetic development in Nlrp2-deficient oocytes of mature adult mice

The observation that Nlrp2 was abundant in oocytes prompted us to investigate its significance for early embryogenesis. Oocytes from superovulated *Nlrp2*$^{-/-}$ mice and WT controls were collected and analyzed for their developmental potential upon parthenogenetic activation with strontium chloride (Ma et al., 2005). Oocytes of 6–10-wk-old *Nlrp2*$^{-/-}$ mice—approximating young adult age in humans—progressed through the two-cell, four-cell, and morula embryonic stages with normal efficiency (Fig. 4, a and b) and kinetics (Fig. 4 c), with ∼30% of both Nlrp2-sufficient and -deficient oocytes having adopted the morphological appearance of blastocysts 5 d after parthenogenetic activation (Fig. 4, a–c). However, *Nlrp2*$^{-/-}$ oocytes from mice aged 22–25 wk—which approximates mature adult age in humans—progressed asynchronously and with significantly reduced rates through the four-cell and morula stages (Fig. 5, a–c). This contrasted markedly with oocytes from similarly aged WT mice, close to 80% of which successfully developed into blastocysts (Fig. 5 c). Instead, most *Nlrp2*$^{-/-}$ embryos were lost or appeared fragmented by day 5, and <10% reached the blastocyst stage (Fig. 5). Despite the striking age-associated defect in early embryogenesis, metaphase II–arrested oocytes collected from both 6–10- and 22–25-wk-old *Nlrp2*$^{-/-}$ mice had spindles of seemingly normal size and shape (Fig. S2, a–d). Also spindle-mediated chromosome segregation appeared to be grossly normal when analyzed 1 h after parthenogenetic

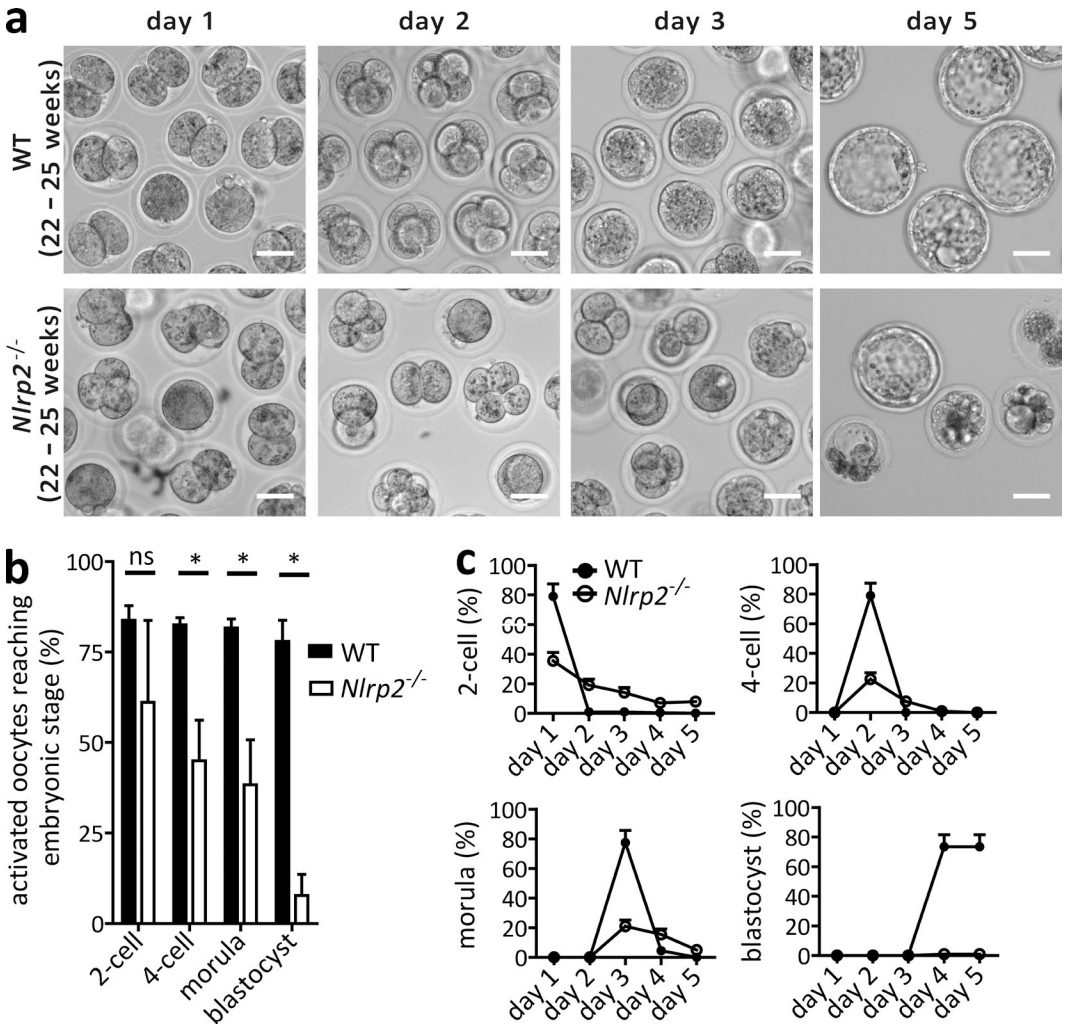

Figure 5. **Nlrp2 is required for efficient parthenogenetic development of oocytes from mature adult mice.** (a) Representative bright field micrographs of developing embryos at days 1, 2, 3 and 5 after parthenogenetic activation of oocytes obtained from 22–25 wk old WT and *Nlrp2*$^{-/-}$ mice. (b) Fraction of activated oocytes from 22–25 wk old WT and *Nlrp2*$^{-/-}$ mice that reached the indicated embryonic cleavage stages. (c) Kinetic analysis of the progression of activated oocytes from 22–25 wk old WT and *Nlrp2*$^{-/-}$ mice through the indicated embryonic cleavage stages. Data represent mean ± SD of 301 oocytes from 17 WT mice, and 207 oocytes from 17 *Nlrp2*$^{-/-}$ mice. (ns, nonsignificant; *, $P < 0.05$; Student's *t* test). Bars, 50 µm.

activation (Fig. S2, e and f). Many genes that contribute importantly to early embryogenesis in mammals are subject to imprinting, an epigenetic process of gene silencing in reproductive cells that allows selective expression of alleles in a parent-of-origin–dependent manner (Van Gorp et al., 2014). Given that the nucleotide sequences of Nlrp2 transcripts of C57BL/6J, BALB/c, and 129S1 mice are fully conserved in their open reading frames (unpublished data), naturally encoded Nlrp2 mRNA variants could not be exploited to distinguish maternal- and paternal-derived Nlrp2 transcripts in oocytes. We therefore took advantage of the differential Nlrp2 alleles of WT and *Nlrp2*$^{-/-}$ mice to establish whether Nlrp2 was imprinted (Fig. S3 a). After breeding *Nlrp2*$^{-/-}$ females to *Nlrp2*$^{+/+}$ males, RT-PCR analysis of oocytes of the resulting heterozygous offspring showed the presence of transcripts corresponding to both the WT and knockout *Nlrp2* alleles (Fig. S3 b), indicating that *Nlrp2* is not imprinted because both the parental and maternal *Nlrp2* alleles were actively transcribed. Together, these results suggest that Nlrp2 regulates early embryogenesis after oocyte activation.

Nlrp2 regulates maternal fertility in vivo

Although more work is needed to pinpoint the molecular mechanisms involved, the aforementioned findings led us to hypothesize that Nlrp2 may exert a role in vivo in early embryogenesis that gains significance with progressing maternal age. To empirically address this possibility, WT and *Nlrp2*$^{-/-}$ females were bred to randomly selected WT and *Nlrp2*$^{-/-}$ males when aged 7 wk, and their reproductive performance was monitored over time until they became 45 wk old. No-

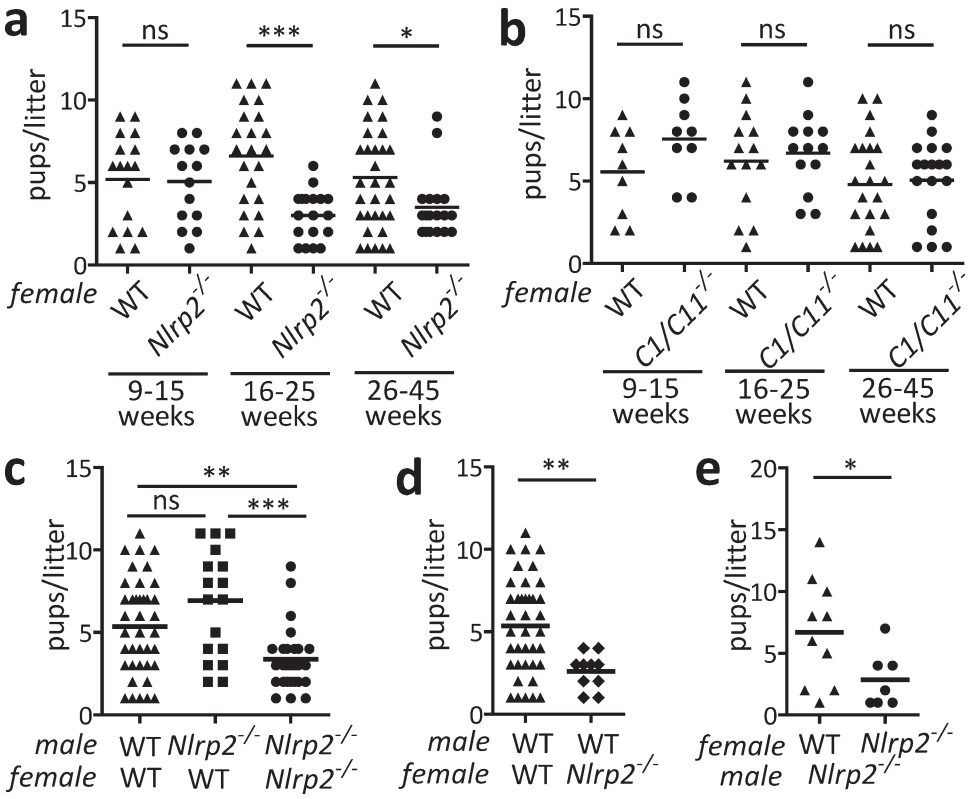

Figure 6. **NLRP2 selectively controls maternal age-associated fertility in vivo.** (a) WT (n = 14) and *Nlrp2*$^{-/-}$ (n = 10) female mice were randomly bred to WT (n = 5) and *Nlrp2*$^{-/-}$ (n = 7) males when aged 7 wk, and size of each litter was determined until they were 45 wk of age. (b) WT (n = 8) and *Casp1*$^{-/-}$*Casp11*$^{-/-}$ (*C1/C11*$^{-/-}$; n = 8) female mice were bred when aged 7 wk to WT (n = 4) and *Casp1*$^{-/-}$*Casp11*$^{-/-}$ (n = 5) males, respectively, and size of each litter was determined until they were 45 wk of age. (c) WT (n = 5) and *Nlrp2*$^{-/-}$ (n = 7) male mice aged >16 wk were bred to either WT or *Nlrp2*$^{-/-}$ females as indicated, and litter size was determined over time. (d) WT (n = 8) and *Nlrp2*$^{-/-}$ (n = 2) female mice aged >16 wk were bred to WT males, and litter size was determined over time. (e) *Nlrp2*$^{-/-}$ males of proven fertility (n = 4) were each placed in a separate cage and bred to one randomly selected WT and 1 *Nlrp2*$^{-/-}$ female aged >14 wk. Litter size was determined by genotypic assignment of pups to female mice in the respective cages. Data represent mean ± SD (ns, nonsignificant; *, P < 0.05; **, P < 0.01; ***, P < 0.001; Student's t test).

tably, litters were comparably sized when WT and *Nlrp2*$^{-/-}$ females were 9–15 wk old, but *Nlrp2*$^{-/-}$ females delivered significantly less pups/litter as they grew older (Fig. 6 a). Nlrp2 likely controls maternal fertility independently of inflammasomes because females lacking the central inflammasome proteases caspases 1 and 11 did not have reduced litter sizes with progressing age (Fig. 6 b). We next addressed whether the in vivo role of Nlrp2 in regulation of age-associated fertility extended to males. To this end, *Nlrp2*$^{-/-}$ and WT males that were aged >16 wk were mated with WT females of similar age to compare the reproductive performance of these breeding couples. *Nlrp2*$^{-/-}$ males had litter sizes that were comparable to those of WT males (Fig. 6 c), whereas a control group of *Nlrp2*$^{-/-}$ males that was mated to *Nlrp2*$^{-/-}$ females showed a significant reduction in the number of pups delivered per litter (Fig. 6 c). We also performed a reciprocal experiment in which WT males were bred to either WT or *Nlrp2*$^{-/-}$ females. In agreement with our other findings, *Nlrp2*$^{-/-}$ females had markedly less pups per litter relative to their WT counterparts (Fig. 6 d). These results confirm that Nlrp2 selectively controls maternal fertility in mature adult mice. To further validate and expand on these findings in a controlled setting, four *Nlrp2*$^{-/-}$ males of proven fertility were each co-housed with one randomly selected WT and one *Nlrp2*$^{-/-}$ female of >14 wk old. Litter sizes in this experiment were determined based on genotype of the pups with all heterozygous pups in the breeding cage being assigned to the WT female, and *Nlrp2*$^{-/-}$ pups being born from the knockout female. In agreement with our other observations, we found that litters of mature adult *Nlrp2*$^{-/-}$ females were significantly smaller than those of WT females (Fig. 6 e), confirming that Nlrp2 is required for optimal fertility with progressing maternal age.

In conclusion, we showed here that Nlrp2 selectively controls maternal age-associated fertility. Together with the reported sterility of female mice with a hypomorphic Nlrp5 allele (Tong et al., 2000), our results define a growing subset of NLRs with demonstrated in vivo roles in maternal fertility. Defective Nlrp5 causes female sterility as a result of an oocyte-intrinsic inability to de-

velop beyond the two-cell embryonic stage, whereas the results presented here implicate Nlrp2 in an oocyte-intrinsic developmental checkpoint that gains significance with progressing maternal age. These findings set the experimental context for future studies aimed at elucidating the molecular mechanisms through with NLRP2 controls early embryogenesis. Among other possibilities, Nlrp2 may be a maternal effect gene that directly or indirectly supports proper imprinted gene expression patterns and pluripotency of developing zygotes under ovarian age-associated stress conditions (Barton et al., 1984; Van Gorp et al., 2014). Defective NLRP2 signaling may thus affect reproductive function in patients. Indeed, anecdotal evidence links mutations in human *NLRP2* with increased susceptibility to reproductive disorders, such as sporadic Beckwith-Wiedemann syndrome (Meyer et al., 2009) and Silver–Russell syndrome (Court et al., 2013). Moreover, humans encode a second (primate-specific) Nlrp2 orthologous gene, *NLRP7*, that is frequently found mutated in patients with familial cases of biparental molar pregnancies (Nguyen and Slim, 2014; Van Gorp et al., 2014). As increased maternal age is a prime factor driving the fast-growing societal demand for in vitro fertilization and other assisted reproductive technologies, our findings additionally support examination of whether *NLRP2* and *NLRP7* polymorphisms impact on embryo quality and success rates in these patient groups. Thus, this work sheds light on the role of Nlrp2 as a critical checkpoint of early preimplantation embryogenesis, and warrants investigation of defective NLRP2 and NLRP7 function in women with early menopause manifestation and other conditions associated with declining maternal fertility.

MATERIALS AND METHODS

Mice

Nlrp2$^{floxNeo+}$ mice were generated at Ingenious Targeting Laboratory Inc. by conditional targeting of exon 5 in C57BL/6 embryonic stem (ES) cells. Resulting chimeras were bred to Flp-transgenic mice to delete the FLP recombinase target (FRT) sequences-flanked neomycin selection cassette. Nlrp2-deficient mice were obtained after breeding to appropriate Cre recombinase-expressing mice. *Casp1*$^{-/-}$*Casp11*$^{-/-}$ mice have been reported (Kuida et al., 1995). All mice were housed under specific pathogen–free conditions, and animal studies were conducted under protocols and guidelines approved by the Ghent University animal care and use committee (ECD14/74; ECD15/02).

Genotyping

The following primers were used for genotyping *Nlrp2*$^{-/-}$ mice: R1, 5′-CCTGGTGAATCCAATGTCTAGG-3′; F1, 5′-GGAGCCCTGATGATTCTTTGG-3′; F2, 5′-CTGAAGTCTCTCATTCTCTATAGG-3′. *Nlrp2*$^{+}$ (primers R1, F2), 406 bp; *Nlrp2*^{flox} (primers R1, F2), 583 bp; and *Nlrp2*$^{-}$ (primers R1, F1), 691 bp.

Oocyte collection and parthenogenetic activation

Females of the indicated age and genotypes were superovulated by i.p. injection of pregnant mare serum gonadotropin (PMSG; 5 IU; Folligon; Intervet), 48 h later followed by i.p. injection of human chorionic gonadotrophin (hCG; 5 IU; Chorulon; Intervet). Mice were euthanized, cumulus-enclosed oocytes were recovered and treated with hyaluronidase (0.3 mg/ml; H4272; Sigma-Aldrich) in M2 media (M7167-50ML; Sigma-Aldrich) to remove cumulus cells. Oocytes were then washed and maintained in KSOM (MR-121-D; EMD Millipore) in an incubator (at 37°C and 5% CO_2) for 2 h. Subsequently, oocytes were incubated in Ca^{2+}-free HTF media containing $SrCl_2$ (10 mM) and cytochalasin D (2 µg/ml; C8273; Sigma-Aldrich). 4 h later, embryos were washed and cultured further in KSOM medium in a 5% CO_2 incubator at 37°C. Morulas were transferred to blastocyst media (K-SIBM-50; Cook Medical). Developing embryos were analyzed under 20× objective of IX71 inverted Microscope by CCD Camera XM-10 (Olympus) with resolution 0.6442 µm/pixel in Imaging software CellB (Olympus).

Immunofluorescence microscopy

Oocytes were collected from oviducts of superovulated mice, transferred to extraction/fixation solution (200 µl 50 mM Hepes, 4% paraformaldehyde, 0.2% Triton X-100, 5 mM $MgCl_2$, 5 mM EGTA, pH 7.4, and 0.1 M PIPES, pH 7.4, in water) in 9-well Pyrex plates (13-748B; Thermo Fisher Scientific) and incubated at room temperature for 1 h before incubation in 200 µl blocking solution (PBS; BSA [4%] and Tween [0.25%]) for an additional 1 h. Oocytes were stained with an α-tubulin antibody (1:200; T9026; Sigma-Aldrich) in blocking solution, washed, and incubated with a donkey anti–mouse IgG conjugated to Alexa Fluor 488 (A-21202; Thermo Fisher Scientific). Mounted samples were visualized under a TCS SP5 (Leica) and confocal microscopes. Spindle length was measured after 3D reconstruction of 2-µm z-stacks using Imaris software.

RNA extraction and first strand synthesis

RNA was extracted from mouse tissues using RNeasy mini kit (74104; QIAGEN) according to the manufacturer's protocol. RNA concentration was measured using a NanoDrop ND-8000, and cDNA was synthesized using QuantiTect Reverse Transcription kit (205311; QIAGEN) according to the manufacturer's instructions.

RT-PCR

The following primers were used for RT-PCR analysis: Nlrp2F: 5′-CCCTGAAAGTAGAAAAGGCGG-3′; Nlrp2R: 5′-CCACTTTCTGGAGACAACAGG-3′; Nlrp9bF: 5′-TCAGATGTATTATCAGTGACTGC-3′; Nlrp9bR: 5′-GGAGACATCGAATTACAGAGG-3′; Nlrp5F: 5′-GCTGCTGATTAACCAGAAGATGG-3′; Nlrp5R: 5′-GGCCCGTTGACTCAGGATGC-3′; Nlrp14F: 5′-GCTCAGCCATACCTTGAAGC-3′; Nlrp14R: 5′-CTCCAGCTCCTG

AAGATTGC-3′. Nlrp2 cDNAs were amplified for imprinting analysis with the following primers: Nlrp2R2: 5′-AAA AATGAAATGAGGAAGAGGAGG-3′; Nlrp2F2: 5′-AGT GAAAGCTGGTGTGGTGG-3′. Phusion Hot Start Flex 2X Master Mix (M0536L; NEB) was used for PCR amplification.

qRT-PCR

qRT-PCR was performed on a mouse normal tissue qPCR array (MNRT301; Origene) with the LightCycler 480 SYBR Green I Master (4707516001; Roche) and the following primers: NLRP2F: 5′-CCCTGAAAGTAGAAA AGGCGG-3′; Nlrp2R: 5′-CCACTTTCTGGAGACAAC AGG-3′; GapdhF: 5′-GGTGAAGGTCGGTGTGAACG-3; GapdhR: 5′-CTCGCTCCTGGAAGATGGTG-3′. Nlrp2 expression levels were normalized to Gapdh.

Cell culture and reagents

BMDMs and DCs were prepared as previously described (Vande Walle et al., 2014). The following reagents were used as indicated: FSL-1 (100 ng/ml; tlrl-fsl; InvivoGen), Pam3CSK4 (100 ng/ml; tlrl-pms; InvivoGen), *S. minnesota* LPS (100 ng/ml or 500 ng/ml; tlrl-smlps; InvivoGen), nigericin (20 µM, N7143-10MG; Sigma-Aldrich), *C. difficile* toxin B (1 µg/ml; #155L; List Biological Laboratories); Lipofectamine-2000 (5 µl; 11668–019; Invitrogen), Fugene (E2311; Promega). $CD4^+$ T cells were purified by negative selection with $CD4^+$ T cells isolation kit II (130–095-248; Miltenyi Biotec) according to manufacturer's instructions. $CD4^+$ T cell were activated with plate-bound anti-CD3 (4 µg/ml; 14–0031-85; eBioscience) and anti-CD28 antibodies (1 µg/ml; 14–0281-82; eBioscience), or with PMA (100 ng/ml; P1585-1MG; Sigma-Aldrich) together with ionomycin (1 µg/ml; I0634; Sigma-Aldrich).

Cytokine and cell death assays

Cytokines were analyzed with Luminex (Bio-Rad Laboratories) and ELISA (R&D Systems) assays according to guidelines of the manufacturers. Cell death was determined by lactate dehydrogenase (LDH) assay (G1780; Promega).

Western blotting

Cell lysates and culture supernatants were incubated with 1X Caspase Lysis Buffer (0.1% NP-40, 20 mM NaCl, 2 mM Tris-HCl, pH 7.4) on ice and denatured in Laemmli buffer. Samples were boiled and separated by SDS-PAGE. Separated proteins were transferred to PVDF membranes. Blocking, incubation with antibody, and washing of the membrane were done in PBS supplemented with 0.05% Tween-20 (vol/vol) and 3% (wt/vol) nonfat dry milk. Immunoblots were incubated overnight with primary antibodies against caspase-1 (AG-20B-0042-C100; 1:1,000; Adipogen), followed by HRP-conjugated secondary anti–mouse antibodies (1:5,000; 115–035-146; Jackson ImmunoResearch Laboratories) to detect proteins by enhanced chemiluminescence (Thermo Fisher Scientific).

Flow cytometry

Cells from primary and secondary immune organs were prepared by mechanical dissociation through 70-µm cell strainers (08–771-2; Corning). 1–5 million cells were blocked with anti-mouse CD16/CD32 antibody (14–0161-85, eBioscience), and stained with anti-TCRβ-biotin (13–5961-81, eBioscience) followed by incubation with SA-APC (17–4317-82; eBioscience,) and anti-CD19-PE (12–0193-81, eBioscience) for spleen and LN cells; anti-B220-PE (12–0452-82; eBioscience) for BM cells; anti-CD4-FITC (11–0041-82; eBioscience) and anti-CD8-APC (17–0081-81; eBioscience) for thymocytes; and anti-CD11b-APC (17–0112-81; eBioscience), anti-GR1-FITC (11–5931-82; eBioscience) and anti-CD11c-PE (12–0114-81; eBioscience) for myeloid cells in the presence of propidium iodide for analysis of cell death. Cells were analyzed on a FACSCalibur (BD) machine.

Statistical analysis

Statistical analyses were performed using the Student's *t* test in GraphPad Prism5 software. $P < 0.05$ was considered statistically significant.

Online supplemental material

Fig. S1 describes production and genotyping of *Nlrp2*$^{-/-}$ mice. Fig. S2 shows normal spindle morphology in *Nlrp2*$^{-/-}$ oocytes. Fig. S3 shows that *Nlrp2* is not imprinted. Table S1 shows that *Nlrp2*$^{-/-}$ mice are born with expected Mendelian ratios from heterozygous parents.

ACKNOWLEDGMENTS

The authors thank the VIB Bio Imaging core for assistance with imaging, and Dr. Marnik Vuylsteke for statistical analysis support.

This work was supported by European Research Council grant 281600, the Fund for Scientific Research-Flanders grant G011315N, and the Baillet Latour Medical Research grant to M. Lamkanfi.

The authors declare no competing financial interests.

Author contributions: A.A. Kuchmiy and M. Lamkanfi designed the study; A.A. Kuchmiy, J. D'Hont, and T. Hochepied performed experiments; A.A. Kuchmiy, J. D'Hont, T. Hochepied, and M. Lamkanfi analyzed data. A.A. Kuchmiy and M. Lamkanfi wrote the manuscript with input from the other authors, and M. Lamkanfi oversaw the project.

Submitted: 13 June 2016
Revised: 27 September 2016
Accepted: 24 October 2016

REFERENCES

Agostini, L., F. Martinon, K. Burns, M.F. McDermott, P.N. Hawkins, and J. Tschopp. 2004. NALP3 forms an IL-1β-processing inflammasome with increased activity in Muckle-Wells autoinflammatory disorder. *Immunity.* 20:319–325. http://dx.doi.org/10.1016/S1074-7613(04)00046-9

Barton, S.C., M.A. Surani, and M.L. Norris. 1984. Role of paternal and maternal genomes in mouse development. *Nature.* 311:374–376. http://dx.doi.org/10.1038/311374a0

Bruey, J.M., N. Bruey-Sedano, R. Newman, S. Chandler, C. Stehlik, and J.C. Reed. 2004. PAN1/NALP2/PYPAF2, an inducible inflammatory mediator that regulates NF-κB and caspase-1 activation in macrophages.

J. Biol. Chem. 279:51897–51907. http://dx.doi.org/10.1074/jbc.M406741200

Court, F., A. Martin-Trujillo, V. Romanelli, I. Garin, I. Iglesias-Platas, I. Salafsky, M. Guitart, G. Perez de Nanclares, P. Lapunzina, and D. Monk. 2013. Genome-wide allelic methylation analysis reveals disease-specific susceptibility to multiple methylation defects in imprinting syndromes. *Hum. Mutat.* 34:595–602. http://dx.doi.org/10.1002/humu.22276

Fontalba, A., O. Gutierrez, and J.L. Fernandez-Luna. 2007. NLRP2, an inhibitor of the NF-kappaB pathway, is transcriptionally activated by NF-κB and exhibits a nonfunctional allelic variant. *J. Immunol.* 179:8519–8524. http://dx.doi.org/10.4049/jimmunol.179.12.8519

Geddes, K., J.G. Magalhães, and S.E. Girardin. 2009. Unleashing the therapeutic potential of NOD-like receptors. *Nat. Rev. Drug Discov.* 8:465–479. http://dx.doi.org/10.1038/nrd2783

Kanneganti, T.D., M. Lamkanfi, and G. Núñez. 2007. Intracellular NOD-like receptors in host defense and disease. *Immunity.* 27:549–559. http://dx.doi.org/10.1016/j.immuni.2007.10.002

Kinoshita, T., Y. Wang, M. Hasegawa, R. Imamura, and T. Suda. 2005. PYPAF3, a PYRIN-containing APAF-1-like protein, is a feedback regulator of caspase-1-dependent interleukin-1β secretion. *J. Biol. Chem.* 280:21720–21725. http://dx.doi.org/10.1074/jbc.M410057200

Kuida, K., J.A. Lippke, G. Ku, M.W. Harding, D.J. Livingston, M.S. Su, and R.A. Flavell. 1995. Altered cytokine export and apoptosis in mice deficient in interleukin-1 β converting enzyme. *Science.* 267:2000–2003. http://dx.doi.org/10.1126/science.7535475

Lamkanfi, M., and V.M. Dixit. 2012. Inflammasomes and their roles in health and disease. *Annu. Rev. Cell Dev. Biol.* 28:137–161. http://dx.doi.org/10.1146/annurev-cellbio-101011-155745

Lamkanfi, M., and V.M. Dixit. 2014. Mechanisms and functions of inflammasomes. *Cell.* 157:1013–1022. http://dx.doi.org/10.1016/j.cell.2014.04.007

Lupfer, C., and T.D. Kanneganti. 2013. The expanding role of NLRs in antiviral immunity. *Immunol. Rev.* 255:13–24. http://dx.doi.org/10.1111/imr.12089

Ma, S.F., X.Y. Liu, D.Q. Miao, Z.B. Han, X. Zhang, Y.L. Miao, R. Yanagimachi, and J.H. Tan. 2005. Parthenogenetic activation of mouse oocytes by strontium chloride: a search for the best conditions. *Theriogenology.* 64:1142–1157. http://dx.doi.org/10.1016/j.theriogenology.2005.03.002

Meyer, E., D. Lim, S. Pasha, L.J. Tee, F. Rahman, J.R. Yates, C.G. Woods, W. Reik, and E.R. Maher. 2009. Germline mutation in NLRP2 (NALP2) in a familial imprinting disorder (Beckwith-Wiedemann Syndrome). *PLoS Genet.* 5:e1000423. http://dx.doi.org/10.1371/journal.pgen.1000423

Nguyen, N.M., and R. Slim. 2014. Genetics and epigenetics of recurrent hydatidiform moles: Basic science and genetic counselling. *Curr. Obstet. Gynecol. Rep.* 3:55–64. http://dx.doi.org/10.1007/s13669-013-0076-1

Peng, H., B. Chang, C. Lu, J. Su, Y. Wu, P. Lv, Y. Wang, J. Liu, B. Zhang, F. Quan, et al. 2012. Nlrp2, a maternal effect gene required for early embryonic development in the mouse. *PLoS One.* 7:e30344. http://dx.doi.org/10.1371/journal.pone.0030344

Peng, H., X. Lin, F. Liu, C. Wang, and W. Zhang. 2015. NLRP9B protein is dispensable for oocyte maturation and early embryonic development in the mouse. *J. Reprod. Dev.* 61:559–564. http://dx.doi.org/10.1262/jrd.2015-050

Ting, J.P., S.B. Willingham, and D.T. Bergstralh. 2008. NLRs at the intersection of cell death and immunity. *Nat. Rev. Immunol.* 8:372–379. http://dx.doi.org/10.1038/nri2296

Tong, Z.B., L. Gold, K.E. Pfeifer, H. Dorward, E. Lee, C.A. Bondy, J. Dean, and L.M. Nelson. 2000. Mater, a maternal effect gene required for early embryonic development in mice. *Nat. Genet.* 26:267–268. http://dx.doi.org/10.1038/81547

Vande Walle, L., N. Van Opdenbosch, P. Jacques, A. Fossoul, E. Verheugen, P. Vogel, R. Beyaert, D. Elewaut, T.D. Kanneganti, G. van Loo, and M. Lamkanfi. 2014. Negative regulation of the NLRP3 inflammasome by A20 protects against arthritis. *Nature.* 512:69–73.

Van Gorp, H., A. Kuchmiy, F. Van Hauwermeiren, and M. Lamkanfi. 2014. NOD-like receptors interfacing the immune and reproductive systems. *FEBS J.* 281:4568–4582. http://dx.doi.org/10.1111/febs.13014